

RECEIVED 2001 AUGUST 31; ACCEPTED 2001 SEPTEMBER 24

Preprint typeset using L<sup>A</sup>T<sub>E</sub>X style emulateapj

## LOCATING THE STARBURST IN THE SCUBA GALAXY, SMM J14011+0252

R. J. Ivison<sup>1</sup>, Ian Smail<sup>2</sup>, D. T. Frayer<sup>3</sup>, J.-P. Kneib<sup>4</sup> & A. W. Blain<sup>5</sup>

Received 2001 August 31; accepted 2001 September 24

## ABSTRACT

We present new, multi-wavelength, high-resolution imaging of the luminous, submillimeter (submm) galaxy, SMM J14011+0252, an interacting starburst at  $z = 2.56$ . Our observations comprise optical imaging from the *Hubble Space Telescope*, sensitive radio mapping from the Very Large Array and CO observations from the Owens Valley Radio Observatory and Berkeley-Illinois-Maryland Array. Aided by well-constrained gravitational amplification, we use these new data to map the distribution of gas and both obscured and unobscured starlight. The maps show that the gas and star formation are extended on scales of  $\gtrsim 10$  kpc, much larger than starbursts seen in local ultraluminous galaxies, and larger than the rest-frame UV-bright components of SMM J14011+0252, J1/J2. The most vigorous star formation is marked by peaks in both the molecular gas and radio emission,  $\sim 1''$  north of J1/J2, in the vicinity of J1n, an apparent faint extension of J1. Using new sub-0.5'' *K*-band imaging from UKIRT, we identify J1n as an extremely red object (ERO). We suggest that while J1 and J2 are clearly associated with the submm source, they are merely windows through the dust, or unobscured companions to a large and otherwise opaque star-forming system. Hence, their rest-frame UV properties are unlikely to be relevant for understanding the detailed internal physics of the starburst.

*Subject headings:* cosmology: observations — galaxies: individual (SMM J14011+0252; SMM J14009+0252) — galaxies: evolution

## 1. INTRODUCTION

The resolution into individual sources of the majority of the optical, submm and X-ray backgrounds (Madau & Pozzetti 2000; Blain et al. 1999; Brandt et al. 2001) means that we can now investigate the relationship and balance between obscured and unobscured star formation and AGN activity at high redshifts. For example, the limited overlap between X-ray and submm populations has been taken as evidence that the bulk of the submm background arises from reprocessed starlight (Fabian et al. 2000; Barger et al. 2001; Almaini et al. 2001). While the broad equality between the intensity of the optical and far-IR background radiation has then been used to argue that comparable amounts of star formation occur in obscured and unobscured environments (Hauser et al. 1998). A major unresolved issue is the relationship between the obscured and unobscured modes of star formation, as represented by SCUBA-selected galaxies and Lyman-break galaxies, respectively (Smail, Ivison, & Blain 1997; Steidel, Pettini, & Hamilton 1995). Is unobscured activity simply the tip of the iceberg, and can it be used to predict the obscured component (Adelberger & Steidel 2000), or do Lyman-break galaxies represent a physically distinct population with no meaningful relationship with galaxies selected in the submm (van der Werf et al. 2001; Meurer et al. 2001; also see Bell et al. 2001)? This has important implications for the relative contributions of optical- and submm-selected galaxies to the history of star formation (Blain et al. 1999b; Chapman et al. 2000; Peacock et al. 2001).

To address this issue we need to study the properties of individual submm galaxies. Unfortunately, progress has been con-

strained by their faintness in the rest-frame UV and the resultant dearth of spectroscopic redshifts and detailed morphologies for more than a handful of systems (Ivison et al. 1998, 2000a — I00). For the moment all we have to work with are a few, perhaps atypical, optically-bright galaxies with precise redshifts. There are also concerns about the over-representation of AGN in the current samples of spectroscopically-identified submm galaxies, reflecting a bias from the relative ease of measuring redshifts for their strong-lined spectra. Although star formation, rather than the AGN, is thought to dominate the energetics of these systems, the presence of an AGN clearly complicates any detailed analysis. We are therefore left with only a single example from current surveys of the class of galaxy which is expected to comprise the majority of the submm population: the  $z = 2.56$ , gas-rich, luminous starburst, SMM J14011+0252 (I00), although even this appears unusually bright in the rest-frame UV.

SMM J14011+0252, lying behind the core of the  $z = 0.25$  cluster A 1835, has an 850- $\mu$ m flux of 6 mJy, after correcting for amplification by the foreground cluster lens (a mean factor of  $2.5\times$ , dominated by amplification along position angle  $9^\circ$ ), showing that this is an ultraluminous IR galaxy (ULIRG) with a far-IR luminosity of  $L_{\text{FIR}} \sim 6 \times 10^{12} L_\odot$ , a star-formation rate (SFR) of  $\sim 10^3 M_\odot \text{ yr}^{-1}$  and a large dust mass,  $M_d \sim 10^8\text{--}10^9 M_\odot$ . I00 present detailed observations of this submm-selected source, which they identified with an interacting/merging pair of galaxies, J1 and J2, separated by  $2.1''$ , with a combined absolute magnitude of  $M_R = -25.0^6$ . J2 contributes the bulk of the luminosity in the UV, with the red-

<sup>1</sup>Astronomy Technology Centre, Royal Observatory, Blackford Hill, Edinburgh EH9 3HJ, UK<sup>2</sup>Department of Physics, University of Durham, South Road, Durham DH1 3LE, UK<sup>3</sup>SIRTF Science Centre, California Institute of Technology, IPAC, MS 220-06, Pasadena, CA 91125, USA<sup>4</sup>Observatoire Midi-Pyrénées, UMR 5572, 14 Avenue E. Belin, F-31400 Toulouse, France<sup>5</sup>Astronomy 105-24, California Institute of Technology, Pasadena, CA 91125, USA

<sup>6</sup>Throughout we will assume  $q_0 = 0.5$  and  $H_0 = 50 \text{ km s}^{-1} \text{ Mpc}^{-1}$ , giving a scale of  $1'' \equiv 7.7 \text{ kpc}$  at  $z = 2.56$ . We quote all magnitudes and linear scales as observed, rather than corrected for lens amplification, unless otherwise stated.

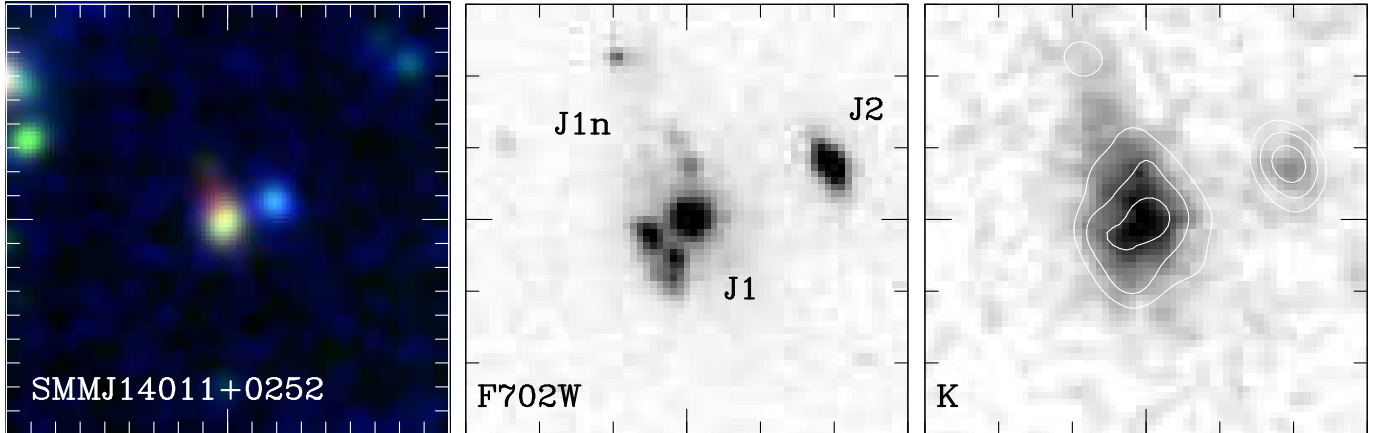


FIG. 1.— Three views of SMM J14011+0252: a true-color  $UR_{702}K$  image (using  $U$ -band data from I00), the *HST* F702W frame and the UKIRT  $K$ -band image. The true-color frame is  $18'' \times 18''$ , while the F702W/ $K$ -band views are zoomed to give a  $6'' \times 6''$  field to better illustrate the internal structure of this galaxy. We identify the two UV-bright components of SMM J14011+0252 on the F702W panel: the morphologically complex J1 and the compact, blue component J2, as well as the diffuse, very red component, J1n. We overlay a contour plot of the seeing-matched F702W image on the  $K$ -band panel to contrast the optical/IR morphologies (the contours are in 1-mag increments starting at  $\mu_R = 24.0 \text{ mag arcsec}^{-2}$ ). North is up; east is left; minor tickmarks denote  $1''$  increments.

der J1 dominating the near-IR. Optical and near-IR spectra of J1 and J2 show no hint of AGN characteristics (I00) and the system is undetected in hard X-ray observations with *Chandra* (Fabian et al. 2000), supporting the contention that its luminosity is predominantly produced by an intense starburst. The accurate redshift for this system allowed Frayer et al. (1999) to detect CO(3→2) emission, confirming the presence of a large gas reservoir,  $M(\text{H}_2) \sim 10^{11} \text{ M}_\odot$  (probably a lower limit based on evidence of cold gas from CO(1→0) emission in another source, Papadopoulos et al. 2001).

Although the observational dataset on SMM J14011+0252 is the most comprehensive available for any submm galaxy, there is still considerable freedom in interpreting the results. In particular, we need to identify the location of the intense far-IR emission within the system, and the attendant gas reservoir, to understand the exact relationship between the UV and far-IR emission (Adelberger & Steidel 2000) and determine if they are coming from physically disjoint components. Unfortunately, the published observations had insufficient spatial resolution to answer this question. We have therefore undertaken a campaign to image SMM J14011+0252 at high resolution in the radio, millimeter (CO) and optical/near-IR wavebands to investigate in detail the distribution of obscured and unobscured star formation in this galaxy.

We describe our new high-resolution images in §2, analyse these in §3 and present our conclusions in §4.

## 2. OBSERVATIONS AND REDUCTION

### 2.1. Optical and Near-IR Imaging

The *HST*<sup>7</sup> imaging of SMM J14011+0252, in the field of A1835, comprises three orbits in the F702W filter, giving a combined integration time of 7.5 ks. We adopt the Vega-based *WFPC2* photometric system,  $R_{702}$ , from Holtzman et al. (1995). The final *WFPC2* frame (see Fig. 1) has an effective resolution of  $0.15''$  and a  $3\sigma$  detection limit within a  $2''$ -diameter pho-

tometry aperture of  $R_{702} \sim 26.6$ . We also exploit new, near-IR imaging of SMM J14011+0252. Using UFTI on the UKIRT,<sup>8</sup> Smith et al. (2001) obtained a 6.5-ks  $K$ -band exposure during 2001 April 4–7. The image (Fig. 1c) has a  $3\sigma$  limit of  $K \sim 21.2$  and a FWHM of  $0.45''$ . The reduction and analysis of both the *HST* and UKIRT data is described in full in Smith et al. (2001).

### 2.2. Centimeter and Millimeter Mapping

The initial Owens Valley Millimeter Array (OVRO)<sup>9</sup> CO observations taken of J1/J2 in 1998 showed evidence for a possible extended component in the north-south direction (Frayer et al. 1999). We subsequently obtained 78 hr of high-resolution CO observations at OVRO and the Berkeley-Illinois-Maryland Array (BIMA)<sup>10</sup> to constrain the CO morphology and position of the source (Table 1).

TABLE 1  
MILLIMETER OBSERVATIONS OF SMM J14011+0252

Observing Dates	Array	Baseline Lengths (m)	Time on Source (h)	RMS (mJy)	$\theta_b^a$ (''')
1998 Oct–Dec	OVRO(L+E)	15–119	41.4	1.0	$6.5 \times 4.3$
1999 Dec	BIMA(A)	80–1730	16.7	2.0	$0.7 \times 0.6$
2000 Feb–Mar	OVRO(H+U)	35–483	19.8	1.8	$2.4 \times 1.9$

<sup>a</sup> The rms and synthesized beam sizes ( $\theta_b$ ) are for a natural-weighted map averaged over the CO line width of  $320 \text{ km s}^{-1}$ . The data were taken in four OVRO configurations (L, E, H, U) and the highest resolution BIMA configuration (A).

Fig. 2a shows the integrated CO map of the combined OVRO and BIMA data. In order to resolve the galaxy while maintaining good signal to noise, we adopt a natural-weighting scheme with a UV taper of  $120 k\lambda$  using AIPS. We achieved an rms noise level  $0.8 \text{ mJy beam}^{-1}$  integrated over the CO emission-line width of  $320 \text{ km s}^{-1}$ , with a beam of  $3.9'' \times 3.9''$ .

The A 1835 field was also mapped with the National Radio Astronomy Observatory's (NRAO) Very Large Array (VLA),<sup>11</sup> during 1998 April and 2000 November. After standard calibration and editing of the data and their associated weights using

<sup>7</sup>This paper is based upon observations obtained with the NASA/ESA *Hubble Space Telescope* which is operated by STScI for the Association of Universities for Research in Astronomy, Inc., under NASA contract NAS5-26555.

<sup>8</sup>The United Kingdom Infrared Telescope (UKIRT) is operated by the Joint Astronomy Centre on behalf of the Particle Physics and Astronomy Research Council.

<sup>9</sup>OVRO is operated by the California Institute of Technology and is supported by NSF grant AST 9981546.

<sup>10</sup>The BIMA array is operated by the Berkeley-Illinois-Maryland Association under funding from the NSF.

<sup>11</sup>NRAO is operated by Associated Universities Inc., under a cooperative agreement with the National Science Foundation.

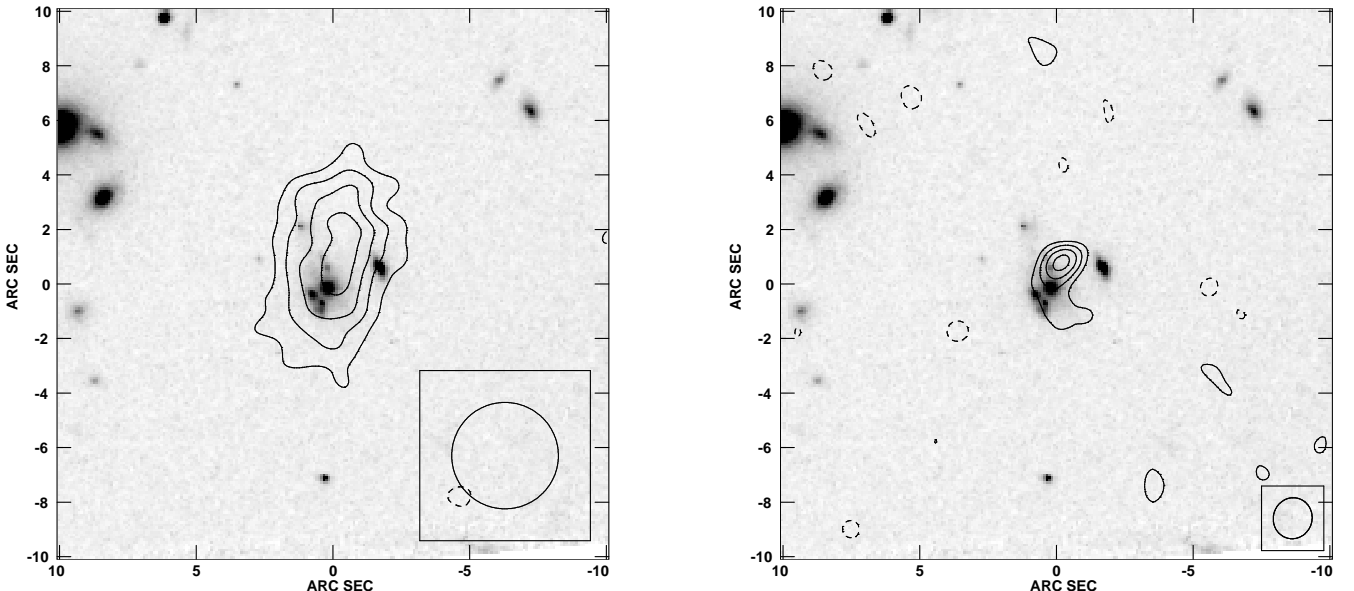


FIG. 2.— (a) Combined OVRO/BIMA CO image of SMM J14011+0252, with a noise level of  $0.8 \text{ mJy beam}^{-1}$ ; (b) VLA 1.4-GHz map, with a noise level of  $12 \mu\text{Jy beam}^{-1}$ . The CO and radio emission are co-spatial, peaking  $\sim 1''$  north of J1. The CO subtends  $6.6'' \pm 1.4''$  in the north-south direction, the radio somewhat less. All contours are plotted at  $-3.5, -2.5, 2.5, 3.5, 4.5, 5.5 \times \sigma$ ; positions are relative to the position of J1, shown as a greyscale; synthesized beams are shown.

AIPS, the wide-field imaging task, IMAGR, was used to map the central  $10' \times 10'$  field (see, e.g. Richards 2000). The resulting map (Fig 2b) has a noise level of  $12 \mu\text{Jy beam}^{-1}$  with  $1.45''$  resolution.

### 2.3. Astrometry

To reliably compare the positions of the components of SMM J14011+0252 we have revisited the astrometry from I00 to tie the optical and near-IR images directly to the radio coordinate frame. By identifying bright radio sources within the *HST* field we align the frames to a precision of  $\sim 0.3''$ . We then measure the position of J1 to be  $14^{\text{h}}01^{\text{m}}04^{\text{s}}95 \pm 0^{\text{s}}02, +02^{\circ} 52' 24.0 \pm 0.3''$  (J2000).

The peak of the 1.4-GHz radio source lies at  $14^{\text{h}}01^{\text{m}}04^{\text{s}}92, +02^{\circ} 52' 24.8''$  (J2000), with an uncertainty of  $\pm 0.2''$ , coincident with the CO emission which peaks at  $14^{\text{h}}01^{\text{m}}04^{\text{s}}93, +02^{\circ} 52' 25.0''$  (J2000), with an uncertainty of  $\pm 0.7''$ .

## 3. ANALYSIS AND DISCUSSION

The *HST* imaging of SMM J14011+0252, aided by the gravitational amplification from A 1835, provides a sub-kpc scale view of the components of this submm source in the rest-frame UV,  $\sim 2000 \text{ \AA}$ . This shows that J1 is well resolved, with a half-light diameter of  $1.34'' \pm 0.08''$  ( $3.3 \pm 0.2 \text{ kpc}$  in the source plane). As with another submm galaxy, Lockman 850.1 (Lutz et al. 2001), its morphology is complex: the main component appears to be relatively regular, with an extended envelope. Superimposed on this are several bright knots, in two groups: one to the south-east and the other to the north (which also appears in *K*). The northern group points towards another bright, resolved blue knot,  $2.5''$  away. This knot defines the outer limit of a low-surface-brightness extension, J1n, to the north of J1, which has an extent of  $10 \text{ kpc}$  in the source plane and which is much more prominent in *K* than *R* (Fig. 1). We note, as did

Ivison et al. (1998), that red plumes such as this may be due to line emission: probably  $\text{H}\alpha$  at  $2.34 \mu\text{m}$  (I00), which could be mapped in the future using near-IR integral-field spectroscopy.

The second bright component, J2, is more luminous than J1 at rest-frame wavelengths of  $\lesssim 2000 \text{ \AA}$ , but rapidly becomes fainter in redder wavebands. J2 has a compact appearance, with a half-light diameter of  $0.50'' \pm 0.06''$ . The morphology of J2 suggests it could be an edge-on disk extending out to  $\sim 0.5''$ , with a high-surface-brightness nucleus, though the prominence of this extension may result from the higher north-south amplification.

Photometry from the seeing-matched F702W and *K*-band frames gives: J1,  $(R_{702} - K) = 3.29 \pm 0.03$  and J2,  $(R_{702} - K) = 2.12 \pm 0.05$ , both in apertures twice the size of their respective half-light diameters. J1n is much redder than either of the bright components with  $(R_{702} - K) = 5.03 \pm 0.10$ , very similar to the extreme colors seen in other submm galaxies<sup>12</sup> (Smail et al. 1999).

As shown in Fig. 2, the peaks of the CO and radio emission in our high-resolution maps lie  $\sim 1''$  north of J1 and  $\sim 2''$  east of J2. Given the precision of our astrometry, these offsets are significant and so we can rule out the starburst arising from either of these components. The radio/CO emission are not coincident with the ERO, J1n, but are more consistent with this component than with any other. Thus the bulk of the luminosity, gas and dust appear to be located close to, or within, the extremely red component.

I00 estimated the SFR for  $\geq 8 M_{\odot}$  stars in SMM J14011+0252, based on far-IR and radio fluxes, of  $\sim 10^3 M_{\odot} \text{ yr}^{-1}$ . In contrast, the  $\text{H}\alpha$  luminosity indicates only  $\sim 10^2 M_{\odot} \text{ yr}^{-1}$ . They concluded that the likely cause of this discrepancy is significant dust extinction, extending to rest-frame  $\sim 6600 \text{ \AA}$  (observed *K*-band), which obscures the most vigorously star forming regions within the galaxy. This is consistent with the faint appearance of the star-forming region

<sup>12</sup>SMM J14009+0252 is a 14.5-mJy 850- $\mu\text{m}$  source in the same field as SMM J14011+0252. It has a very faint near-IR counterpart (J5) which was, and remains, undetected at optical wavelengths. We can now place a  $3-\sigma$  limit on its color of  $(R_{702} - K) \geq 5.8$  in a  $2''$ -diameter aperture, meaning that this galaxy is an ERO or a Class 0/I submm source (Ivison et al. 2000b). This brings the fraction of EROs in the Smail et al. sample to  $\geq 27$  per cent ( $\geq 44$  per cent for the  $4\sigma$  sample).

in our  $K$ -band image and its complete absence in the  $HST$  frame, as well as the conclusions of studies which contrast the very different appearance of local starbursts in the optical and the near-IR/radio. We suggest that the known optical components, J1/J2, merely represent foreground star-forming knots, or windows through the dust in a large and otherwise opaque star-forming complex.

Since the starburst is obscured even at  $K$ , we must turn to our long- $\lambda$  observations to investigate its morphology. The distributions of both the radio and CO emission are extended roughly north–south, consistent with alignment of J1–J1n, with the emission resolved along this axis. After deconvolving the beam, the molecular gas traced by CO subtends  $6.6'' \pm 1.4''$  along the major axis (Fig. 2a). Assuming conservatively that the amplification is entirely north–south, the molecular gas must cover at least 20 kpc. The best Gaussian fit to the 1.4-GHz emission gives  $2.3'' \times 1.5''$  (FWHM), although a fainter emission extends to the south (Fig. 2b). We stress that several nearby radio sources remain unresolved in our map, so this extension is real. This strongly suggests that the far-IR emission is powered by a starburst: the vast molecular gas reservoir appears to be converted into stars and ultimately into SNe on a galaxy-wide scale. The growing evidence of highly extended starbursts in the submm galaxy population (Ivison et al., in prep) indicates that physical conditions (gas densities, dust shielding, wind formation) in these systems will be very different from those expected on the basis of local, compact ( $\leq 1$  kpc) ULIRGs.

#### 4. CONCLUSIONS

We have presented new high-resolution optical, CO and radio observations of the  $z = 2.56$  SCUBA-selected ULIRG, SMM J14011+0252. Our new  $K$ -band imaging has allowed us to resolve an ERO component within this system ( $R_{702} - K = 5.0$ ). Of the known optical/near-IR components, this heavily dust-obscured component is closest to the starburst, as probed by our high-resolution CO and radio maps.

These observations are relevant for the issue of the relationship between the Lyman-break and submm galaxy populations. In this paper we have studied a galaxy which has been claimed to represent the transition between these two populations, with UV properties that confirm the reliability of large extinction corrections of the type applied to Lyman-break galaxies (Adelberger & Steidel 2000). Our higher resolution data

have demonstrated that the properties of SMM J14011+0252 are much more complex than previously thought, with the bulk of the luminosity coming from an extremely red component which is not seen in rest-frame UV observations, or possibly from a region which is blank even in the near-IR. While the optically bright components, J1 and J2, are clearly associated with the submm source, they appear as distinct regions within the system and their rest-frame UV properties are therefore unlikely to provide a reliable indication of the physical processes occurring within the highly obscured starburst. J1, J2 and even J1n may merely mark windows through the dust in an otherwise opaque star-forming complex. This calls into question the validity of using UV-selected objects to trace the evolution of obscured star formation at high redshifts.

Nevertheless, in the absence of the less obscured components, J1 and J2, this system would have been difficult to study in the detail achieved here. The presence of UV-bright companions may prove to be the only practical way to measure redshifts for submm galaxies for the foreseeable future (see the discussion of J5 in I00; cf. Blain et al. 2000; Townsend et al. 2001).

New information on the luminous submm source, SMM J14009+0252, previously suggested as a radio-loud AGN with ERO characteristics, confirm that this galaxy is an ERO, raising the fraction of known extremely red counterparts to almost half of the most robust parent sample.

High-redshift dusty galaxies such as SMM J14011+0252 and SMM J14009+0252 account for  $\gtrsim 50$  per cent of the submm background (Blain et al. 1999), leaving room for only a modest contribution from the submm counterparts of UV-selected systems (Peacock et al. 2000). This is in sharp contrast to the situation in the local Universe, where very luminous dusty starbursts contribute a minor fraction of the total energy output, underlining the rapid evolution which must occur in the ULIRG population (Smail et al. 1997). Identifying the physical process responsible for this rapid increase in star formation, as well as the reason for the much larger physical scale of high-redshift starbursts compared to local examples, will yield important insights into the formation of massive galaxies.

We thank Leo Blitz, Harald Ebeling, Frazer Owen, Nick Scoville, Graham Smith, Jack Welch and Mel Wright for help and advice. IRS and JPK acknowledge support from the Royal Society, the Leverhulme Trust and CNRS.

#### REFERENCES

Adelberger, K. L., & Steidel, C. C. 2000, ApJ, 544, 218  
 Almaini, O., et al. 2001, MNRAS, submitted (astro-ph/0108400)  
 Barger, A. J., Cowie, L. L., Steffen, A. T., Hornschemeier, A. E., Brandt, W. N., & Garmire, G. P. 2001, ApJ, submitted (astro-ph/0107252)  
 Bell, E. F., Gordon, K. D., Kennicutt, R. C. & Zaritsky, D. 2001, ApJ, submitted (astro-ph/0108367)  
 Brandt, W. N., et al. 2001, AJ, 122, 1  
 Blain, A. W., Kneib, J.-P., Ivison, R. J., & Smail, I. 1999, ApJ, 512, L87  
 Blain, A. W., Frayer, D. T., Bock, J. J., & Scoville, N. Z. 2000, MNRAS, 313, 559  
 Chapman, S., et al. 2000, MNRAS, 319, 318  
 Fabian, A. C., et al. 2000, MNRAS, 315, L8  
 Frayer, D. T., et al. 1999, ApJ, 514, L13  
 Hauser, M. G., et al. 1998, ApJ, 508, 25  
 Holtzman, J. A., et al. 1995, PASP, 107, 156  
 Ivison, R. J., Smail, I., Le Borgne, J.-F., Blain, A. W., Kneib, J.-P., Bézecourt, J., Kerr, T. H., & Davies, J. K. 1998, MNRAS, 298, 583  
 Ivison, R. J., Dunlop, J. S., Smail, I., Dey, A., Liu, M. C., & Graham, J. R. 2000b, ApJ, 542, 27  
 Ivison, R. J., Smail, I., Barger, A., Kneib, J.-P., Blain, A. W., Owen, F. N., Kerr, T. H., & Cowie, L. L. 2000a, MNRAS, 315, 209 [I00]  
 Lutz, D., et al. 2001, A&A, in press (astro-ph/0108131)  
 Madau, P., & Pozzetti, L. 2000, MNRAS, 312, 9  
 Meurer, G. R., Heckman, T. M., Seibert, M., Goldader, J. D., Calzetti, D., Sanders, D., & Steidel, C. C. 2001, pre-print (astro-ph/0011201)  
 Papadopoulos, P., Ivison, R., Carilli, C., & Lewis G. 2001, Nature, 409, 58  
 Peacock, J. A., et al. 2001, MNRAS, 318, 535  
 Richards, E. 2000, ApJ, 533, 611  
 Smail, I., Ivison, R. J., & Blain, A. W. 1997, ApJ, 490, L5  
 Smail, I., Ivison, R. J., Kneib, J.-P., Cowie, L. L., Blain, A. W., Barger, A. J., Owen, F. N., & Morrison, G. 1999, MNRAS, 308, 1061  
 Smail, I., Ivison, R. J., Blain, A. W., & Kneib, J.-P. 2001, MNRAS, submitted  
 Smith, G. P., et al., 2001, MNRAS, submitted  
 Steidel, C. C., Pettini, M., & Hamilton, D. 1995, AJ, 110, 2519  
 Townsend, R. H. D., Ivison, R. J., Smail, I., Frayer, D. T., & Blain, A. W., 2001, MNRAS, submitted (astro-ph/0106112)  
 van der Werf, P., Knudsen, K. K., Labb  , I., & Franx, M. 2001, pre-print (astro-ph/0010459)